

26 May 2010, 4:45 pm - 6:45 pm

Applicability Test of Soil Improvement Using Micro-Bubbles Against Soil Liquefaction

Koichi Nagao
Sato Kogyo Co., Ltd., Japan

Naoaki Suemasa
Tokyo City University, Japan

Tatsuo Akashi
NILIM, Government of Japan, Japan

Mikio Futaki
Center for Better Living, Japan

Follow this and additional works at: <https://scholarsmine.mst.edu/icrageesd>



Part of the [Geotechnical Engineering Commons](#)

Recommended Citation

Nagao, Koichi; Suemasa, Naoaki; Akashi, Tatsuo; and Futaki, Mikio, "Applicability Test of Soil Improvement Using Micro-Bubbles Against Soil Liquefaction" (2010). *International Conferences on Recent Advances in Geotechnical Earthquake Engineering and Soil Dynamics*. 21.

<https://scholarsmine.mst.edu/icrageesd/05icrageesd/session01b/21>



This work is licensed under a [Creative Commons Attribution-Noncommercial-No Derivative Works 4.0 License](#).

This Article - Conference proceedings is brought to you for free and open access by Scholars' Mine. It has been accepted for inclusion in International Conferences on Recent Advances in Geotechnical Earthquake Engineering and Soil Dynamics by an authorized administrator of Scholars' Mine. This work is protected by U. S. Copyright Law. Unauthorized use including reproduction for redistribution requires the permission of the copyright holder. For more information, please contact scholarsmine@mst.edu.



Fifth International Conference on

Recent Advances in Geotechnical Earthquake Engineering and Soil Dynamics and Symposium in Honor of Professor I.M. Idriss

May 24-29, 2010 • San Diego, California

APPLICABILITY TEST OF SOIL IMPROVEMENT USING MICRO-BUBBLES AGAINST SOIL LIQUEFACTION

Koichi NAGAO

Sato Kogyo Co.,Ltd.
Atsugi, Kanagawa, JAPAN

Naoaki SUEMASA

Tokyo City University
Setagaya, Tokyo, JAPAN

Tatsuo AKASHI

NILIM, Government of Japan
Tsukuba, Ibaraki, JAPAN

Mikio FUTAKI

Center for Better Living
Tsukuba, Ibaraki, JAPAN

ABSTRACT

The purpose of this paper is to demonstrate the effectiveness of micro-bubble water injection method against soil liquefaction based on the result of seismic vibration test using large scale flexible shaking box.

It is well known that soil resistance to liquefaction increases as the degree of saturation of the soil decreases, but the practical method to decrease the saturation of the soil has not been invented. The authors solved this problem by new method of injecting water containing micro-air bubbles into the ground. The method has an advantage which not only simple and cost-effective but also friendly to environment.

We examined two cases, which are micro-bubble water injected sand ground and degassed water injected one, to compare the behavior of anti-liquefaction in the large scale test ground soil. As the result, it was observed that liquefaction did not occur even at maximum acceleration level of 200Gal under the condition of lowered saturation to 80% with N-value of around 7, which is loose or fragile ground.

In addition, the results also could be suggested that the possibility of brand new method of “seismic avoid ground” with hybrid layered ground of air injected soil around housing foundations and liquefaction soil under the ground.

INTRODUCTION

Soil liquefaction is a major engineering interest for the geotechnical engineers in the earthquake countries. In Japan, because the most part of built-up area is concentrated on the alluvial plain and soft ground, the soil liquefaction is one of the latent threats.

As for liquefaction countermeasures done in a housing area, ecological aspect and easy maintenance in addition to the cost effectiveness and the compactness of construction will be required.

Though various kinds of liquefaction countermeasures have been developed and performed until now, they have some mutual problems as follows. Most of the countermeasures are difficult to use in a narrow place where existing structures such as housing are standing close together. Also, costs of those countermeasures are quite expensive, because they are required to perfectly prevent from the soil liquefaction.

It is well known that liquefaction resistance of a soil increases as the saturation degree of the soil decreases (Yoshimi et al.1988), so that it is reasonable to say that the saturation decreased ground would be able to prevent seismic damage on buildings and infrastructures.

Therefore, it can be prospected that the anti-liquefaction method using air injection into the ground would be effective solution to the problems such as cost, space and pre-standing housings. In addition, using micro-bubble water which is the brand-new method proposing in this paper is expected to be one of the most practical measure for air injection into the ground with low cost simple equipments without removal of existing structures. Moreover, the air and water is free from contamination as well as friendly to natural environment.

Micro-bubble water is the water containing a lot of air bubbles with a diameter of 10 ~100 micro-meters (Ohnari.2005).

Because of the quite small diameter, the micro-bubble can retain submerged for a few minutes.

The micro-bubble water is usually generated by squirting the water dissolving air out of a nozzle with a small ejection hole under high pressure. In this research, a micro-bubble generator, which can continuously generate the micro-bubble water, produced by Nikuni Corporation, Ltd., was used to supply enough micro-bubble water to a large scaled model ground and fully decrease the saturation degree of the ground.

As mentioned above, it is well known that a soil liquefaction resistance increases as the saturation degree of the soil decreases. However, there have been few experimental cases where enforcing actual observation of the effect on liquefaction resistance by decreasing the saturation degree with actual ground or full scale experiments.

Therefore, in this research, two cases of seismic vibration test using large scale flexible shaking box have been conducted to examine the effectiveness of the micro-bubble injection method.

EXPERIMENTAL METHODOLOGY

SOIL IMPROVEMENT USING MICRO-BUBBLES

Fig. 1 shows the process of decreasing saturation degree of a ground by injecting the micro-bubble water and the mechanism of how the bubbles absorb the increased water pressure by ground shakes.

When the micro-bubble water is injected into between the sand particles of the saturated ground, some of micro-bubbles may pass through the element by the water flowing because the diameter of the bubbles is on the order of 10 micro-meters and less than the size of voids made up by sand particles.

The other micro-bubbles, however, may be trapped at air pockets which are narrow spaces near contact spots between sand particles. The trapped micro-bubble decreases its surface tension and the pressure of the air within the bubble, and grows up to milli-meter size in diameter. Because water surrounding the bubble is highly dissolving the air, the air precipitated into the bubble may help enlarging the bubble.

Though excess pore water pressure tends to be increased by repeated seismic stress, the increased pressure is absorbed by shrinkage of the bubbles.

LARGE SCALE SEISMIC VIBRATION TEST

In the experiment, a large scale shaking table apparatus with a laminated shear box was used, which is owned by the Building Research Institute in Japan (BRI).

An overview of the large scale flexible shaking box is shown in Fig.2. The shaking table is equipped with two actuators which have the ability to activate an inertial load of 450tf at a maximum velocity of 20 cm/s to the horizontal direction.

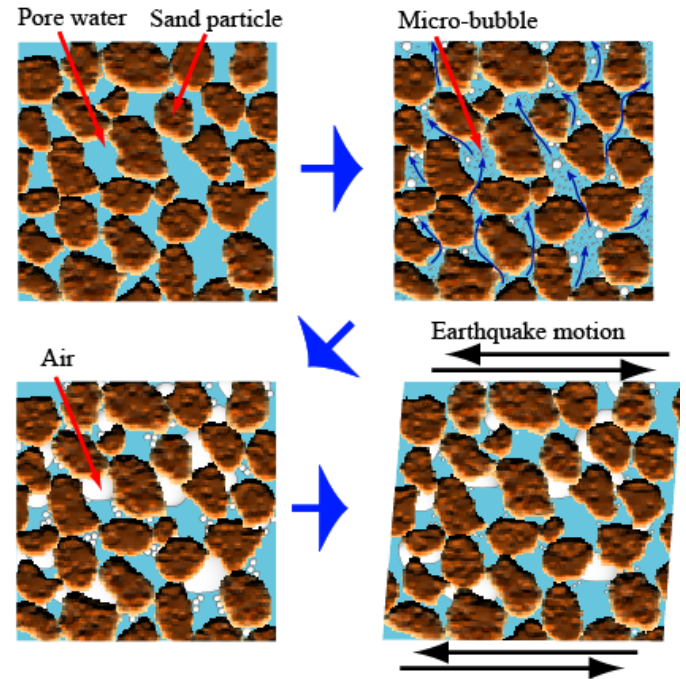


Fig. 1. The process of decreasing saturation of ground by injecting the Micro-bubble water

The laminated shear box, mounted on the shaking table, consists of 17 layers of frames. Each layer with 300 mm height is connected through bearing rollers to the others in order to be independently oscillated. A model ground set up in the box has the sizes of 3.6m wide, 10m long and 5m high.

For the test, Nikko silica sand was used. Physical properties and mechanical properties are indicated Table 1. A grain size accumulation curve of the sand is shown Fig.3. The sand has 7% of fine fraction content, an average grain diameter of 0.25mm and a uniformity coefficient of 2.09.

The model ground was made by filling the wet sand with 250 mm thick and compacting the fill with a compaction roller 4 times for each layer until the ground reached 4,800mm in height. After the complete of filling, a relative density, D_r , of the ground was 44 ~ 46% (45.7% on an average), an N-value was about 7 ~ 13 and the saturation degree was 3 ~ 6%.

For an aim to confirm the effect as the countermeasure for a residential building, a model made by concrete block was put on the surface of the ground, which has sizes of 1.3m by 1.3m, 0.5m in height and weighs 2.5tf so that a contact pressure of the block was 15 kN/m² which is approximately as large as that of an average house.

In the test, two cases of shaking table tests were conducted to access the effect of the countermeasure, in which one was a case injecting the micro-bubble water into the ground (CASE-A) and the other was a case injecting de-aired water (CASE-B). The average condition of test grounds is shown in Table 2. Fig.4 shows liquefaction resistance curves proposed by a series of cyclic triaxial tests for Nikko silica sand and Toyoura sand. Specimens of the tests with 50mm in diameter and 100mm in height were prepared at relative density of about 60% and effective confining pressure, σ_0' was 98kPa. In these test, a cyclic stress ratio to cause double amplitude axial strain, DA, of 5% was defined as the occurrence of liquefaction. Also, the liquefaction resistance of sand was defined as the cyclic stress ratio at which the number of cycles was 20 on the curve.

From Fig.4, it was confirmed that data of cyclic stress ratio for Nikko silica sand were plotted on the liquefaction resistance curves of Toyoura sand regardless of the saturation degree, and the liquefaction resistance of which the saturated degree was 90% by injecting micro-bubble water (MB) was about 1.8 times larger than that of saturated.

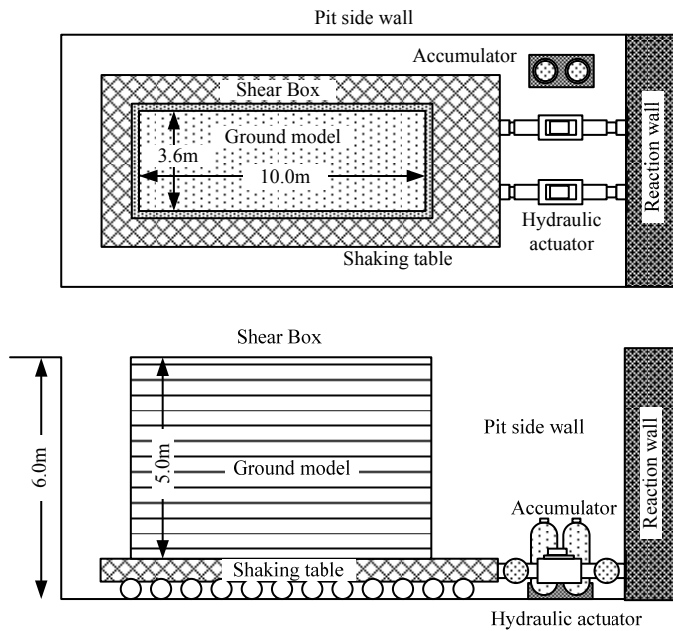


Fig. 2. Large scale flexible shaking box

Table 1. Physical and mechanical properties of Nikko Sand

| | |
|---|--------------------------------|
| Soil particle density ρ_s (t/m ³) | 2.463 |
| Maximum dry density ρ_{dmax} (t/m ³) | 1.698 |
| Minimum dry density ρ_{dmin} (t/m ³) | 1.326 |
| Hydraulic conductivity k_{15} (cm/s) | 2.57x10 ⁻² (Dr=30%) |
| | 1.38x10 ⁻² (Dr=60%) |
| Cohesion C_d (kN/m ²) | 2.6 (Dr=30%) |
| | 0.6 (Dr=60%) |
| Internal friction angle ϕ' (degree) | 31.9 (Dr=30%) |
| | 35.3 (Dr=60%) |

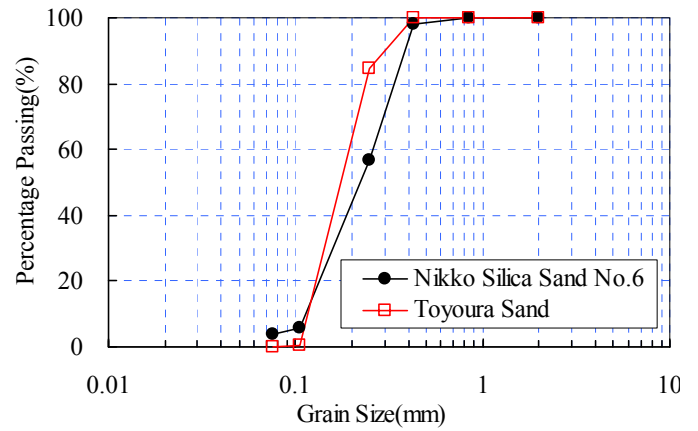


Fig. 3. Grain size accumulation curve

Table 2. Average condition of test ground

| | | CASE-A | CASE-B |
|--|------------------|--------|--------|
| Wet density ρ_t (t/m ³) | | 1.568 | 1.588 |
| Dry density ρ_d (t/m ³) | | 1.474 | 1.469 |
| Relative density Dr (%) | | 45.7 | 44.5 |
| Void ratio e | | 0.79 | 0.80 |
| N-value | Before injection | 6.8 | 6.7 |
| | After injection | 4.8 | 5.9 |

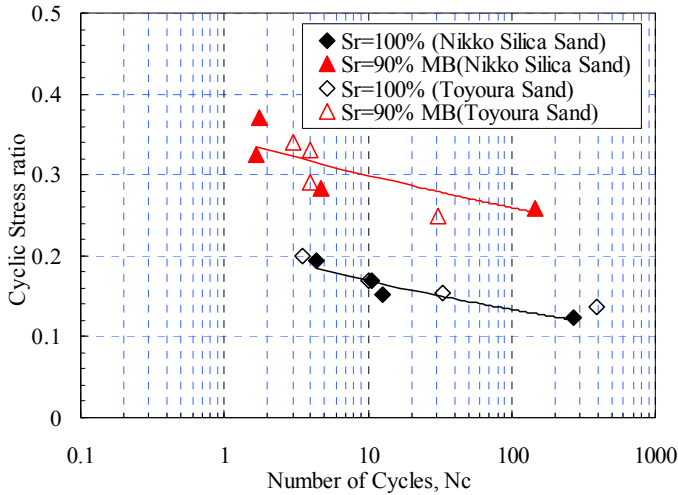


Fig. 4. Liquefaction strength curve

METHOD OF INJECTING INTO THE TEST GROUND

An outline of the micro-bubble water injection system was shown (CASE-A) in Fig.5. The system consists of the micro-bubble generator and a pipe line system to feed the water to the model ground. The micro-bubble generator is mainly composed of a vortex flow turbine pump and an excess air disjoin tank. In the pump, water and air are self-fed by suction of the pump and mixed while the air dissolving in the water. More air dissolution is enhanced under the pressure of the excess air disjoin tank. In the tank, excess air bubbles not to be dissolved are ejected from the tank. The pressurized and air dissolved water from the tank is spurted from injection slits of pipes put on the bottom of the model ground. Then micro-bubbles are precipitated again out of the air dissolved water at the slits.

In the test, a pressure under which the micro-bubble water was generated and pneumatically transported was about 0.6MPa. An inflow of air volume was 5 l/min, and a flow rate of water was 50 l/min. A concentration of dissolved oxygen of the air dissolved water was about 14 mg/l.

Outlines a system for the saturated model ground (CASE-B) is Fig. 6. In the test, de-air water, defined as DO value under 3ppm, was made by using a degassed pump jointed to the micro-bubble system in the condition not to feed the air. Except for this point, the other system for CASE-B was the same as that of CASE-A.

Schematics of arrangements of pipelines and measurement apparatus are described in Fig. 7. 6 injection pipes in each of which has 3 injection slits (check valve) were laid at 1.6m intervals on the floor of the box. Before filling the sand, a flow rate of each pipe was adjusted to be almost the same as the others' by using a controlled valve of each pipe.

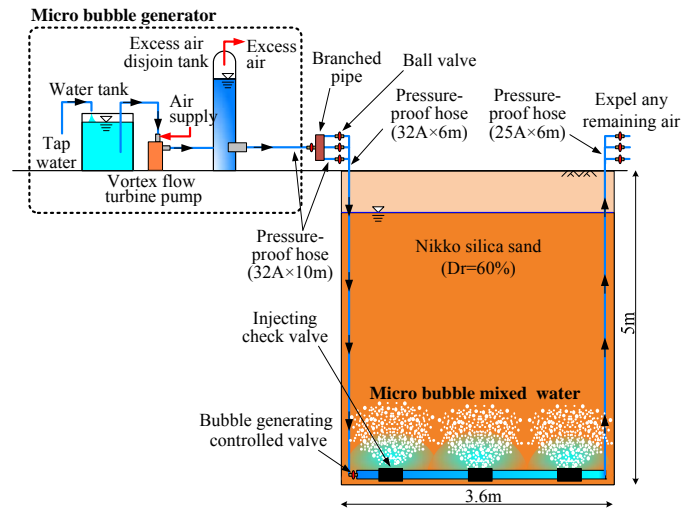


Fig. 5. Outline of Micro-bubble water injection (CASE-A)

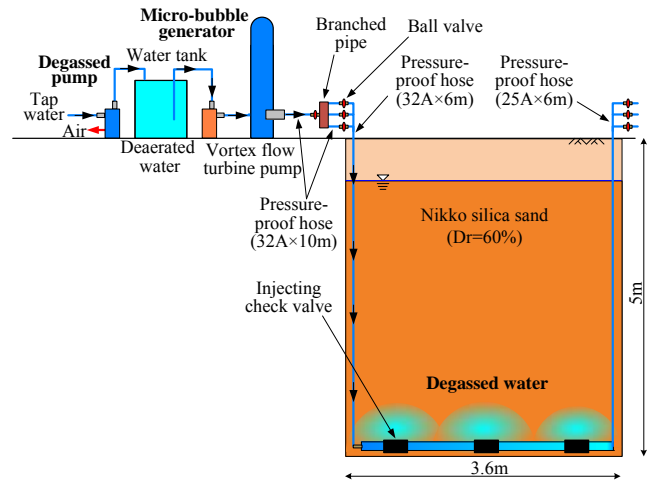


Fig. 6. Outline of Degassed water injection (CASE-B)

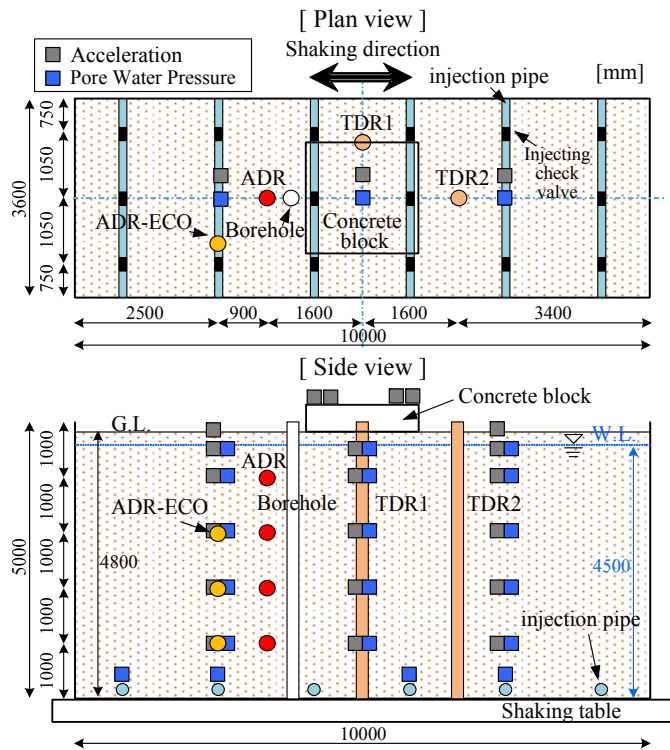


Fig. 7. Arrangements of pipelines and measurements

METHOD OF MEASUREMENT

As shown in Fig. 7, sensors embedded into the model ground were 19 pore water pressure gages, 21 accelerometers and three kinds of dielectric method sensors to measure soil moisture content, including 4 Amplitude Domain Reflectometry (ADR), 3 ADR-ECO and 2 Time Domain Reflectometry (TDR). So the TDR sensor was used, depth distribution of soil moisture content can be obtained by moving the sensor up and down into a special tube embedded.

In addition, to observe the real appearance of air bubbles in the ground and measure stratified data of settlement, a clear acrylic pipe to pilot the borehole CCD camera was set in the ground. Also, ground water level, ground surface level and the settlement and inclination of the weight were measured.

THE TEST RESULT

RESULT OF INJECTING TEST

A change in the degree of saturation measured by ADR sensors during injecting micro-bubble water is indicated in Fig. 8. To convert a volume water content measured by the ADR to the degree of saturation, the following equation was used.

$$\theta = V_w/V = Sr \times e / (1 + e) \quad (1)$$

where θ is a moisture content by volume (%), V_w is a water volume, V is a soil volume, e is void ratio and Sr is the degree of saturation (%).

Fig.9. shows depth distributions of the saturation degree of the model grounds, measured by the TDR after injecting water. In Case-B, though the ground was saturated until 1.5m in height, upper part of the ground than 1.5m couldn't be saturated because of the shortage of passing water. On the other hand, the saturation degree of the ground in Case-A became less than that in Case-B with a difference of 2 ~ 8 %. At least, obvious difference was observed between the parts of ground lower than 2.5m in height. The averages of saturation degree were 79.8% in Case-A and 78.1% in Case-B, respectively.

The existence of air bubbles was observed in Photo 1, taken at the height of around 1.0m before shaking test, and in Photo 2 taken at the same height immediately after shaking test. Dots shining white in the photographs are bubbles. The same scenes were observed as well in the other different depths. Therefore, it was confirmed that micro-bubbles fed in the ground remained as milli-meter sized babbles among soil particles.

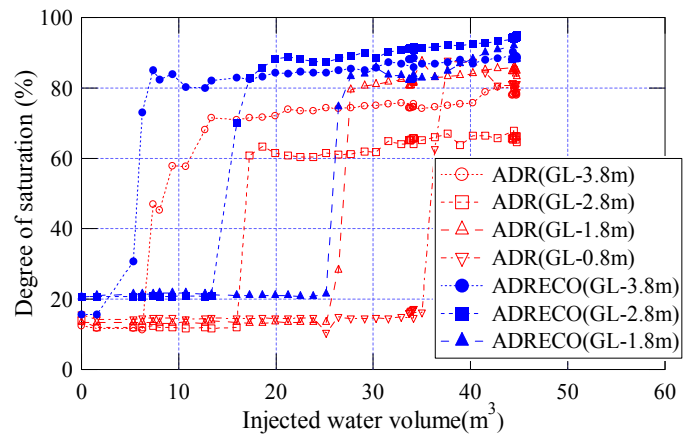


Fig. 8. Change in saturation degree measured by ADR

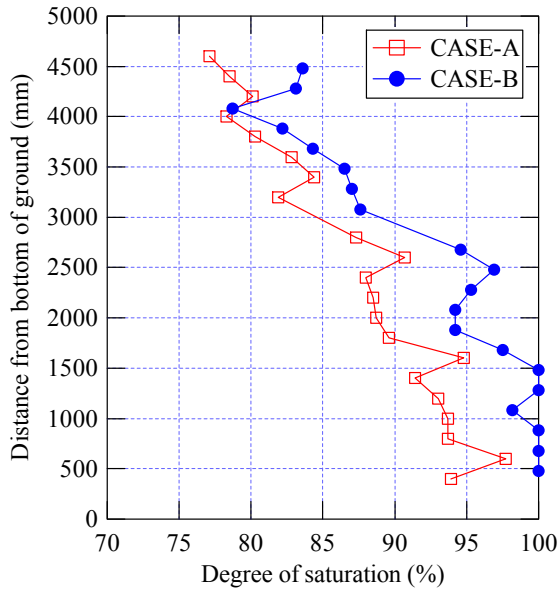


Fig. 9. Distributions of saturation degree measured by TDR



Photo 1. Existence of air bubbles before shaking test



Photo 2. Existence of air bubbles after shaking test

RESULT OF SEISMIC VIBRATION TESTS

The following conditions of oscillation were set up: 20 waves of sinusoidal were used with 2Hz of frequency for one stage, 3 stages of oscillation executed in which maximum acceleration of wave were 50 Gal, 100 Gal, 150 Gal, respectively, executed in the order. In the test, it is noticed that 5 gradual increased waves at the start and 5 gradual decreased waves at the end were added to main shaking waves for control of the actuators. The conditions are described in Table. 3.

The summaries of experiment results are shown in Table 4 for Case-A and Table 5 for Case-B. In the tables, criteria of whether liquefaction occurred or not depended on the ground surface observation after the oscillation ended, such as getting the surface wet or not. According to these results, it can be said that obvious liquefaction wasn't observed apparently in the micro-bubble water injected ground (Case-A) at any oscillation cases except 150 Gal input case which partial liquefaction was observed on the surface.

Observed settlements of the block and the ground surface in Table 6 showed the results, which reverse to the situations that mentioned above. The settlements of the ground surface after the shaking of 150 Gal sank by 41mm in Case-A and 25mm in Case-B, respectively. For the settlements of the block, they were 101mm in Case-A and 37mm in Case-B, respectively. At a glance, this result, CASE-B was hard to be over the damage than CASE-A, was reverse to the expectation.

Horizontal acceleration records for each case are indicated in Fig. 10 and 11. In Case-A, the maximum acceleration at the ground surface was amplified to 180Gal to the input acceleration of 100 Gal, and 210Gal to the 150 Gal input. It was pointed out that considering those acceleration levels, liquefaction of the model ground did not so much observed than usually expected in these amplified levels of accelerations.

Curiously enough, liquefaction wasn't observed both at 100 Gal and 150 Gal oscillations in Case-B, which is high saturated case by degassed water injection. Seeing Fig.11 and Fig.13, it can be seen that both acceleration and water pressure does not fully get through to the surface, especially in case of 150 Gal. Considering the reason of these phenomena, liquefaction was immediately occurred at the bottom part of the ground by the data of rapidly declining acceleration. It was guessed that the immediate liquefaction at the bottom part of the model ground cut liquefaction propagating to the upper part, as if it were seismic avoiding rubber.

The records of the excess pore water pressure are showed in Fig.12 and 13. The maximum pore water pressures in Case-A was smaller than that in Case-B at any depth and shaking level. Also, the increasing rate of the pore pressure in Case-A was smaller, compared with Case-B's results. According to the data, it was also confirmed that the micro-bubble injection could suppress the increase of excess pore water pressure.

In Case-B, as the pore water pressure at the bottom of ground immediately increased, it was seen that liquefaction occurred at that point, where was corresponding to the results of the acceleration. These data also suggests the mechanism on the reason why liquefaction did not be observed on the surface, even on the violent shaking case of 150 Gal input, although it was highly saturated case.

Fig.14 and 15 are contours of the maximum excess pore water pressure ratio at the input acceleration of 100 Gal. According to the contour in CASE-A, liquefaction didn't occur in the whole of ground. Considering that the acceleration of the upper ground was amplified, it came in occurrence of liquefaction at the upper part of the ground. Therefore, it was thought that greater settlement of the block and the ground surface in Case-A was caused by the liquefaction of the upper part of the ground.

In contrast, liquefaction occurred at the lower part of the ground in Case-B. It was said that the excess pore water pressure ratio did not rise in the upper part of the ground, because the acceleration at upper part wasn't amplified by the occurrence of immediate liquefaction at the lower part of the ground. In other words, it was supposed that the liquefaction of lower part played a role of the seismic avoid layer. In addition, it was pointed out that liquefaction at the lower part of ground didn't influence the settlement of the block and the ground surface. Vibration wasn't conveyed to the upper part of the ground in CASE-B.

Table 3. Specification of seismic vibration tests

| | step | frequency | maximum acceleration | wave | wave number |
|--------|------|-----------|----------------------|-----------|-------------|
| CASE-A | 1 | 2.0Hz | 50 Gal | sine-wave | 20 |
| | 2 | | 100 Gal | | |
| | 3 | | 150 Gal | | |
| CASE-B | 1 | 2.0Hz | 50 Gal | sine-wave | 20 |
| | 2 | | 100 Gal | | |
| | 3 | | 150 Gal | | |

Table 4. Summaries of experiment results (CASE-A)

| | | Micro-bubble water | | |
|---------------------------------------|---------|--------------------|---------|---------|
| Degree of saturation (Upper ground) | | 78% | | |
| Maximum acceleration (Shaking table) | | 50 Gal | 100 Gal | 150 Gal |
| Maximum acceleration (Ground surface) | | 80 Gal | 180 Gal | 220 Gal |
| liquefaction | Surface | no | no | liquefy |
| | Bottom | no | no | no |

Table 5. Summaries of experiment results (CASE-B)

| | | Degassed water | | |
|---------------------------------------|---------|----------------|---------|---------|
| Degree of saturation (Upper ground) | | 84% | | |
| Maximum acceleration (Shaking table) | | 50 Gal | 100 Gal | 150 Gal |
| Maximum acceleration (Ground surface) | | 80 Gal | 200 Gal | 160 Gal |
| liquefaction | Surface | no | no | no |
| | Bottom | no | liquefy | liquefy |

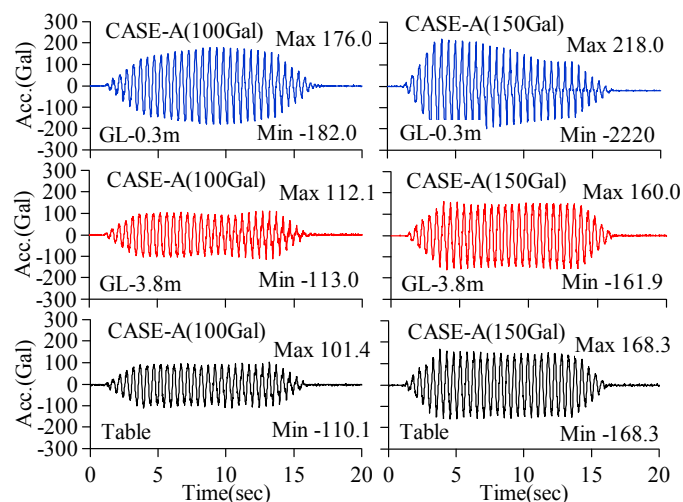


Fig. 10. Acceleration result of the ground (CASE-A)

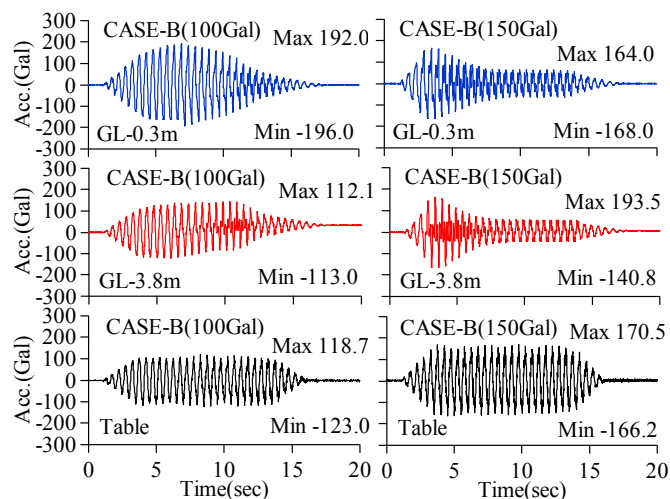


Fig.11. Acceleration result of the ground (CASE-B)

Table 6. Settlements of ground surface and concrete block

| Acceleration | Measure point | CASE-A | CASE-B |
|--------------|----------------|--------|--------|
| 100 Gal | Ground surface | 15mm | 16mm |
| | Concrete block | 20mm | 24mm |
| 150 Gal | Ground surface | 41mm | 25mm |
| | Concrete block | 101mm | 37mm |

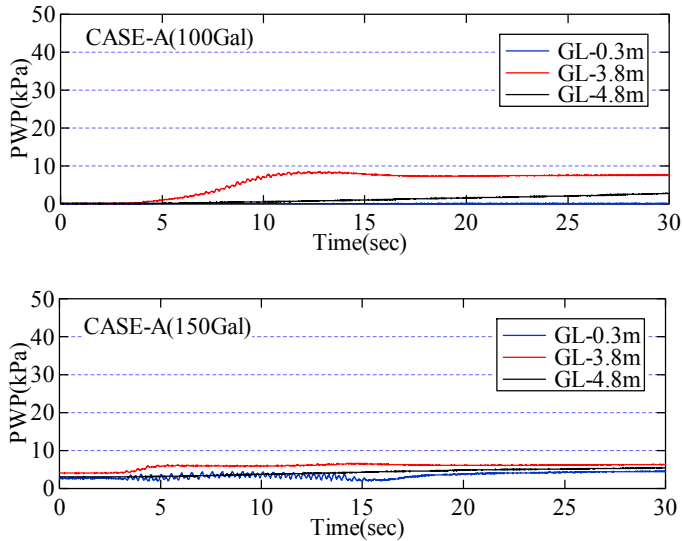


Fig.12 Excess pwp result of the ground (CASE-A)

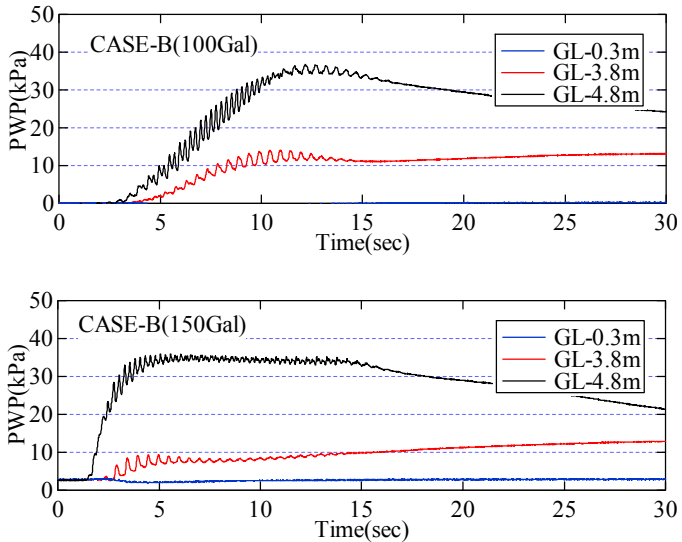


Fig.13 Excess pwp result of the ground (CASE-B)

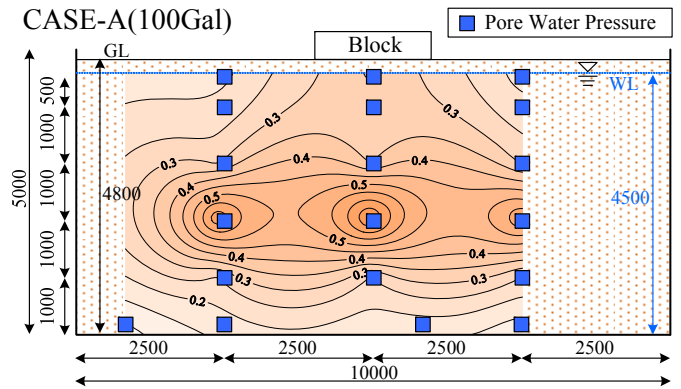


Fig.14 Contour of Maximum excess pwp ratio (CASE-A)

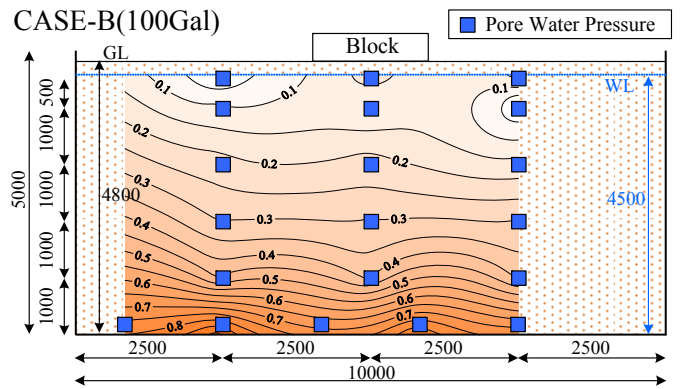


Fig.15 Contour of Maximum excess pwp ratio (CASE-B)

DISCUSSION

Okamura and Soga (2006) brought out the fact that the higher the confining pressure of unsaturated sand become, the larger the liquefaction resistance. It is thought that the liquefaction strength of ground increase about 1.7 times stronger at GL-5m, even if a level of saturation decreases only from 100% to 95%.

As for the seismic vibration test, it is supposed that effect appears more remarkably in the deep position of the ground. Reasonably, terms of vibration with each case are equal at the bottom part of the test ground, because the bottom part performs like shaking table. But on the other hand, the saturation levels are much different in the bottom part because the this part is close to the soil moisture content sensors and the injection points. For these reasons, we compared the results at GL-4.8m.

Fig.16 to 19 show relationships between shear stress ratio obtained by using the acceleration records and the shear strain calculated from horizontal displacement gap between adjacent layers at GL-4.8m. The shear stress τ and the shear strain γ were calculated by the following equations. In addition, the effective overburden pressure σ_z' in GL-4.8m was 43 kPa.

$$\tau = (\rho_i \cdot h \cdot \alpha + M \cdot \alpha / A) / g \quad (2)$$

Where ρ_i is wet density, h is depth, α is acceleration, M is a weight of one shear box step, A is cross-sectional area of shear box and g is gravitational acceleration.

$$\gamma = (D_n - D_{n+1}) / H \quad (3)$$

Where D_n is the amount of horizontal displacement measured at the shear box frame of n th layer, D_{n+1} is the value at $n+1$ th layer and H is the height of the shear box frame.

In Case-B for both shaking of 100 Gal and 150 Gal, the stiffness of the ground showed a nonlinear shape at early stage of the shaking.

On the other hand, in Case-A, the amount of shear strain was smaller than that in Case-B, and the stiffness of the ground was kept in high value until the end of the shaking.

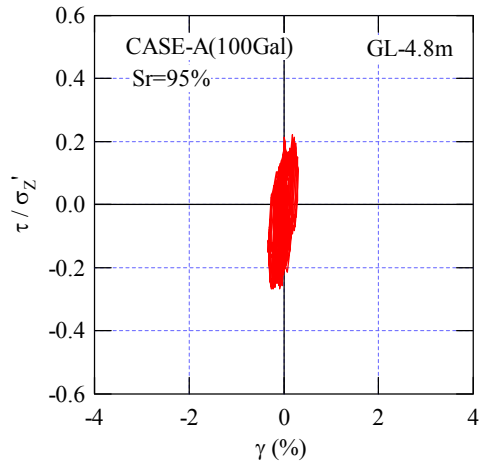


Fig.16 Relationship between τ/σ'_z and γ (CASE-A 100 Gal)

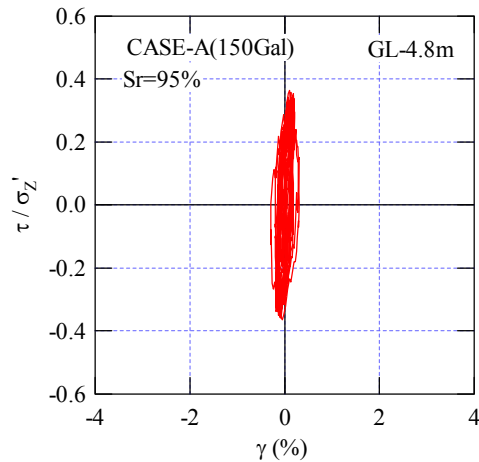


Fig.17 Relationship between τ/σ'_z and γ (CASE-A 150 Gal)

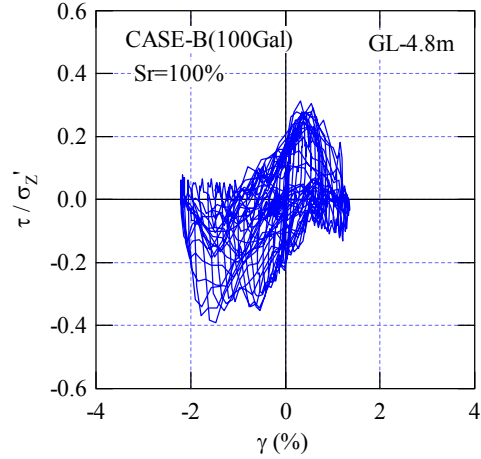


Fig.18 Relationship between τ/σ'_z and γ (CASE-B 100 Gal)

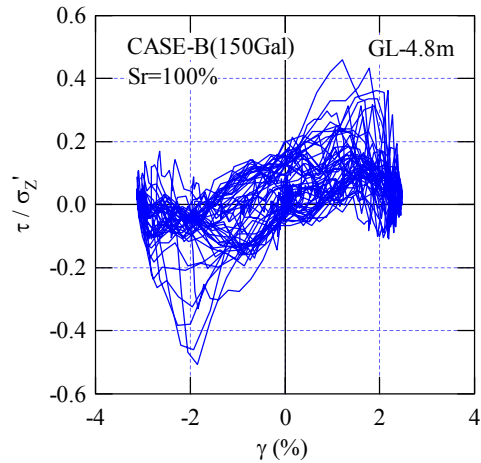


Fig.19 Relationship between τ/σ'_z and γ (CASE-B 150 Gal)

Fig. 20 shows the relationship between the excess pore water pressure ratio observed at GL-4.8m and the number of wave. According to the result, there was almost no change in the pore water pressure in either case of the shaking of 100 Gal or 150 Gal in Case-A.

On the other hand, in Case-B, the pore water pressure was increased as the number of shaking wave become larger, and finally reached the liquefaction condition. Especially in the shaking of 150 Gal, the pore water pressure increased rapidly and liquefied within 6 to 8 waves.

Fig.21 showed the relationship between the maximum shear stress ratio counted at of every 1 wave at GL-4.8m and the number of wave. In Case-B of 150 Gal shaking, the shear stress ratio began to decrease rapidly before the main shaking, and gradually declined with increasing the number of wave. On the other hand, in Case-A, the shear stress ratio kept to be a constant level in the main shaking wave.

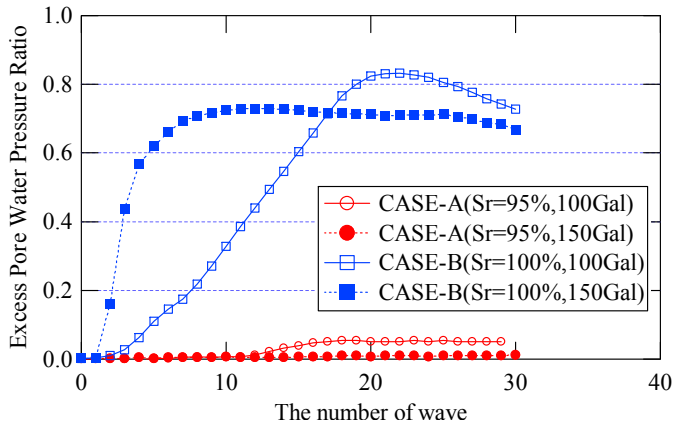


Fig.20 Relationship between excess pwp ratio and number of wave

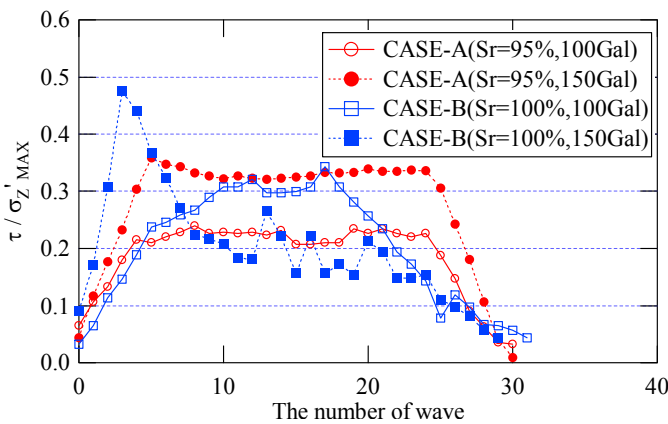


Fig.21 Relationship between $\tau / \sigma'_{z, MAX}$ and number of wave

Fukutake and Mitsuoka (1995) introduced that the strength recovery of undrained cyclic test under the constant pressure was able to be interpreted by using accumulation of shear strain.

As for this test, we used the concept of accumulation of shear strain in order to explain the behavior of the ground in the seismic vibration tests. And also the concept of accumulation of shear stress, at the thought of the damage of the test ground by the cyclic load, was used in the same way.

Fig.22 shows the relationship between the excess pore water pressure ratio and the accumulation of shear strain that counted by every wave. The accumulation of shear strain was calculated by difference between maximum value and minimum value at every wave.

From the early period on accumulation shear strain, the excess pore water pressure ratio of CASE-B is larger than the one of CASE-A, and it is raised more rapidly. And, the excess pore water pressure observed the same tendency despite the size of the input acceleration.

Fig.23 shows the relationship between the excess pore water pressure ratio and the accumulation of maximum shear stress ratio counted at every wave. The accumulation of maximum shear stress ratio was calculated by adding up the maximum shear stress obtained at every wave, which was used as the substitution of cyclic energy. Also, the curves of triaxial test were referred to the existing data of cyclic triaxial tests done for Nikko silica sand, where the relative effective density D_r was 60% and the effective stress σ'_0 was 98kPa.

For most of the curves, the excess pore water pressure ratio increased gradually as the accumulation of shear stress ratios increased. In other words, it was shown that the excess pore water pressure ratio increased with increasing the cyclic energy.

Moreover, the amount of excess pore water pressure ratio in Case-A was smaller than that in Case-B. It showed that the increase of the excess pore water pressure was suppressed by introducing air bubbles in the soil.

The tendency of the results of shaking table tests was the same as that of the cyclic triaxial tests. It suggests that the effect of the air bubble injection on repression of liquefaction was confirmed in large scaled model test as much as shown in the cyclic triaxial test.

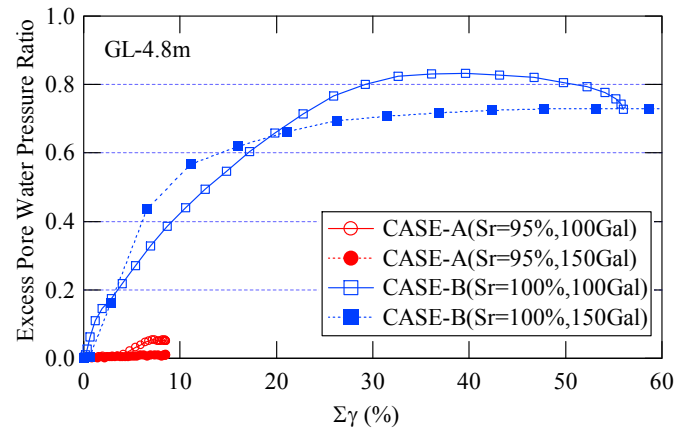


Fig.22 Relationship between excess pwp ratio and $\Sigma\gamma_{MAX}$

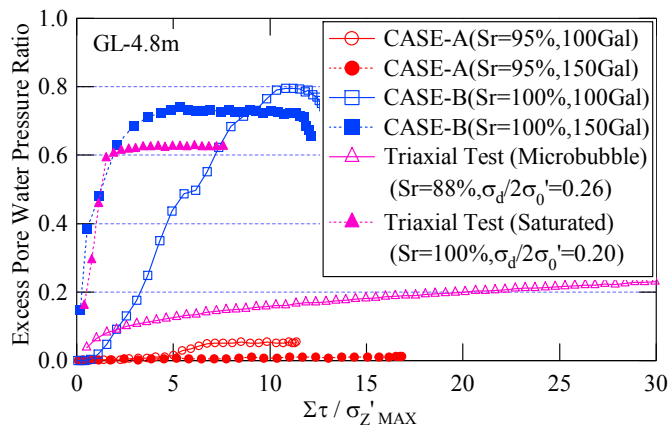


Fig.23 Relationship between excess pwp ratio and $\Sigma\tau/\sigma'_z,MAX$

CONCLUSIONS

According to the result of the seismic vibration tests, the applicability of the micro-bubble water injection method was examined. The conclusions obtained are as follows.

- By examination of injecting micro-bubble water using pipes laid in the bottom of the large scale box of the test sand ground, it was observed that the air was surely stay remained in the test ground soil, and saturation level was decreased around 5% or more compared with degassed water injection ground, which describes the method works well.
- The result also suggests that soil-moisture meter is available to measure the saturation level in the actual ground soil. In addition, air bubbles between the sand particles could be confirmed by using borehole camera.
- By seismic vibration tests, it was observed that liquefaction didn't occur in the condition of maximum acceleration of 200Gal to the lower saturated sand ground of 80% with N-value of around 7, which could say loose or fragile condition.
- In the test sand ground which degassed water was injected, liquefaction occurred in the bottom part of ground immediately after acceleration, and the vibration was absorbed so that it wasn't transmitted to the above of the ground soil, and the surface acceleration became small as the result. On the other hand, in case of the improved test sand ground by micro-bubble water, it was observed that the water pressure level was risen slowly to the top so that the acceleration was amplified at the surface, which is another evidence that the improved ground soil got more strength to resist against seismic input.
- Comparing to the result of cyclic triaxial tests, it is able to say that the result of laboratory test which describe

that micro-bubble water improves staying power against liquefaction is conceivable.

As the conclusion of test, it was found that the method of injecting micro-bubble water into the ground could be a workable countermeasure against soil liquefaction.

In addition, considering the fact that liquefaction ground absorbs seismic power where as lower saturated ground is able to withstand against seismic acceleration up to 200Gal, it could be said that this fact suggest that the possibility of brand new method of "seismic avoid ground" by hybrid layered ground of air injected soil around housing foundation on liquefaction soil ground.

ACKNOWLEDGMENTS

This study and experiment was conducted as a part of the Research Project on "Development of Planning and Management Technologies for the Ultra-long-life Houses and its Site", conducted by National Institute for Land and Infrastructure Management of Japan (NILIM). The authors are grateful to Dr. M.Jinguuji, Dr. M.Okamura, Dr. R.Uzuoka, K.Sugaya, K.Hattori and the other researcher and engineer for help in conducting the experiment in this study, and we also thank students K.Okaniwa and Y.Okada for their help.

REFERENCES

- Fukutake,K. and Mitsuoka,H. [1995]. "A unified law for dilatancy under multi-directional simple shearing". Japan society of civil engineers, No.412, 3-12, pp.143~151.
- Nagao,K., Azegami,Y., Yamada,S., Suemasa,N. and Katada,T. [2007]. "A micro-bubble injection method for a countermeasure against liquefaction". 4th International Conference on Earthquake Geotechnical Engineering, Paper ID 1764, pp.392.
- National Institute for Land and Infrastructure Management. "Development of Planning and Management Technologies for the Ultra-long-life Houses", Internet website, <http://www.nilim.go.jp/engineer/index.html>
- Ohnari,H. [2005]. "Foundation for micro-bubble". Concepts in Basic Bubbles and Foam Engineering, 427-428, 2005
- Okamura,M. and Soga,Y. [2006]. "Effect on liquefaction resistance of volumetric strain of pore fluid". Soil and Foundations, Vol.46,No.5, pp.703~708.
- Tokyo Metropolitan Government. "TMG's Disaster Prevention Information", Internet website, <http://www.bousai.metro.tokyo.jp/english/index.html>

Yoshimi, Y., Tanaka, K. and Tokimatsu, K. [1998].
"Liquefaction resistance of a partially saturated sand". Soils
and Foundations, Vol.29, No.3, 157~600.